NASA-109

RECENT STUDIES OF NONEQUILIBRIUM FLOWS AT THE CORNELL AERONAUTICAL LABORATORY

By

J. Gordon Hall and Anthony L. Russo

Cornell Aeronautical Laboratory, Inc.
Buffalo, New York

12 April 1966

To be presented at the 7th AGARD Colloquium on
Recent Advances in Aerothermochemistry
Oslo, Norway
16-20 May 1966

RECENT STUDIES OF NONEQUILIBRIUM FLOWS AT THE CORNELL AERONAUTICAL LABORATORY

By

J. Gordon Hall* and Anthony L. Russo**

Cornell Aeronautical Laboratory, Inc.
Buffalo, New York

1. INTRODUCTION

The present paper reviews recent work on three problems concerned with nonequilibrium flows carried out in the Aerodynamic Research Department of the Cornell Aeronautical Laboratory. The first problem, discussed in Sec. 2, is that of vibrational relaxation in supersonic nozzle flows of diatomic gases. The initial line-reversal temperature measurements of Hurle, Russo, and Hall[1] for nozzle flows of N_2, which showed unexpectedly fast vibrational relaxation, are first briefly reviewed. Recent confirmatory studies, at other laboratories as well as at CAL, are then described. The results of different investigators for air as well as N_2 are correlated. Line-reversal temperature data recently obtained for nozzle expansions of CO are presented which show fast vibrational relaxation similar to N_2 expansions.

The second problem, discussed in Sec. 3, concerns nonequilibrium effects occurring in high-enthalpy airflows over thick wedge-flat plate bodies where strong (Prandtl-Meyer) flow expansion occurs at the wedge-plate corner. Shock-tunnel experiments and complementary nonequilibrium flow analyses carried out by Vidal and Stoddard[2] on this problem are briefly

*Head, Aerodynamic Research Department
**Principal Mechanical Engineer, Aerodynamic Research Department

described. The experiments indicated substantial nonequilibrium effects on the flat-plate surface pressures. Boundary-layer displacement effects were found to be large following the corner expansion and limited the quantitative interpretation of the data.

The third problem, discussed in Sec. 4, is that of calculating the inviscid nonequilibrium flow field about an Apollo-type re-entry body at arbitrary angle of attack. A time-dependent direct method for this problem is briefly described which has been recently developed by Bohachevsky and Mates[3, 4]. Application by Dunn et al[5] of the ideal-gas solution from this method to estimate nonequilibrium ionization in the Apollo plasma sheath is discussed. Typical results are described for electron density distribution and consequent electromagnetic signal attenuation.

2. VIBRATIONAL RELAXATION OF DIATOMIC GASES IN SUPERSONIC NOZZLE FLOWS*

The experimental study at CAL of the vibrational relaxation of diatomic gases in supersonic nozzle expansions was initially undertaken by the present authors and I. R. Hurle** for N_2 flows[1]. The experimental apparatus consists of a 15° conical nozzle driven by a conventional shock tube. The primary diagnostic technique used is the spectrum-line reversal method which permits the time-resolved measurement of vibrational temperature of the diatomic molecule. Gaydon and Hurle[6] describe the basic principles of the method which is based on the simultaneous measurement of emission

*Various portions of this work were supported by the U. S. Air Force Office of Scientific Research under Contract No. AF 49(638)-792; by the U. S. Air Force Office of Applied Research, Aerospace Research Laboratories, under Contract No. AF 33(657)-8860; and by NASA under Contract NASr-109

**Dr. Hurle is now at Shell Limited, Thornton Research Center, Chester, England.

and absorption intensities of a suitable spectrum line. The intensities are recorded photometrically, and the temperature may be evaluated from the recordings without knowledge of the radiative strength or the density of the emitting species. Resonance lines of Na (5890 Å and 5896 Å) and Cr (4254, 4271, and 4289 Å) are isolated by narrow-band interference filters for the reversal measurements. The Na doublet is resonant with about the 7th vibrational level of N_2, and the Cr triplet is resonant with about the 11th vibrational level of N_2. Details of the shock tube-nozzle and optical apparatus, as well as interpretation of the data, are discussed in Ref. 1, and nozzle-flow calibration studies are described in Ref. 7.

Initial Experiments for Pure N_2 Vibrational Relaxation

Nitrogen vibrational temperature measurements reported in Ref. 1, obtained in the nozzle at area ratios of $A/A^* = 8$ and 32, are shown in Fig. 1. The experimental data shown represent the superposition of the results of many observations for expansions from a reservoir pressure of 50 atm and a reservoir temperature of 4500° K. At these conditions, N_2 dissociation is exceedingly small. The experimental points shown have not been corrected for boundary layer since for this range of conditions the appropriate corrections are small. The curves represent the theoretical vibrational-temperature distributions for equilibrium and nonequilibrium conditions. The lowest curve is the vibrational temperature for complete thermal equilibrium corresponding to zero relaxation time ($\tau = 0$). The upper curve is the vibrational temperature calculated from the Landau-Teller relaxation equation ($\frac{dE}{dt} = \frac{E_\infty - E}{\tau}$, where E = local vibrational energy, E_∞ = local

equilibrium value of the vibrational energy) by a finite difference method using a relaxation time $\tau = \tau_s$. Here, τ_s is the relaxation time used in Ref. 1 as representative of previous studies (e.g., Ref. 14) of vibrational excitation behind shock waves. The three intermediate curves are the predicted vibrational temperature distributions assuming τ = 1/10, 1/15, and 1/20 τ_s. It is emphasized that the shock-wave relaxation times used in these calculations are those given in Fig. 5 of Ref. 1 in contrast with the revised values to be cited later.

It is clear from this figure that the observed vibrational temperatures of N_2 in the nozzle expansion flows lie much closer to equilibrium than predicted by the theory using shock-wave relaxation data. In fact, the experiments indicate that the vibrational de-excitation of N_2 in the nozzle flow proceeds at least one order of magnitude faster than calculated on the basis of shock-wave relaxation times.

The measured temperatures using both Na and Cr are in complete agreement at the area ratio of $A/A^* = 8$. The significance of this observation is that if the exchange of vibrational quanta between levels is not rapid, a non-Boltzmann distribution in vibrational energy becomes possible during the expansion. Such a distribution would not be characterized by a single vibrational temperature and the temperatures inferred from the 11th vibrational level using Cr and from the 7th vibrational level using Na would be different. Thus the agreement of measured vibrational temperatures using Cr and Na support the expectation of rapid vibration-vibration exchange and the existence of a Boltzmann distribution in vibration throughout the relaxation process.

Several experiments were repeated in which no Na or Cr was added to the test gas. In these cases, no detectable light emission or absorption was observed, confirming that the source of radiation was due to Na or Cr atoms, and not to any extraneous effects.

In view of the much shorter vibrational relaxation times indicated by the initial observations, the experimental studies were extended to examine the behavior of the measured vibrational temperatures under various conditions of nozzle-flow pressure and temperature. One series of experiments was conducted at a constant reservoir temperature of 4500° K while the reservoir pressure was varied from 24 to 82 atm. A second series was conducted at a constant reservoir pressure of 50 atm while the reservoir temperature was varied from 2800° to 4600° K. In each of these series of experiments, the measured vibrational temperatures were found to lie closer to equilibrium than values predicted by the relaxation theory using the shock-wave relaxation data. Conversely, the relaxation rates inferred from these data are consistently more than one order of magnitude faster throughout the range of variation of reservoir pressure or temperature than the shock wave results. Further, the nozzle expansion flow results are faster by a constant factor, indicating that the pressure and temperature dependencies of the relaxation process are reasonably well described by the Landau-Teller relaxation theory.

Recent Studies

In view of the significance of the foregoing results to the basic understanding of vibrational nonequilibrium, further experimental studies of this problem have been conducted recently both at CAL and at other laboratories. These additional investigations generally confirm the aforementioned results. Among these studies are: (1) a reconfirmation that the line-reversal technique measures vibrational temperatures in the shock-wave environment[8]; (2) an investigation of the effects of impurities on the vibrational temperature measurements[9]; (3) temperature measurements in dilute-N_2 nozzle expansion flows[10]; (4) measurements of vibrational temperatures in nozzle flows using electron-beam techniques[11, 12] and line-reversal temperature measurements in nonsteady expansion flows[13]; (5) measurements of vibrational temperatures in expansion flows of 5% CO + 95% Ar. Preliminary measurements of line-reversal temperatures in nozzle expansion flows of O_2 have also been obtained. In addition, theoretical studies of vibrational relaxation have been undertaken. These recent studies will now be briefly discussed.

Shock Wave Studies:

Extensive studies of N_2 vibrational relaxation behind shock waves in the temperature range of 1500-5000° K using optical interferometry[14, 15], and infrared emission from trace amounts of CO used as a thermometric element[15], indicated a relaxation time much longer than earlier ultrasonic results for low temperatures, and about two times longer than earlier Na-line reversal results at somewhat higher temperatures[6]. These observations reflected on the shock-wave relaxation times (τ_s) used for the

theoretical calculations of Fig. 1 and, more important, on the interpretation of the Na-line reversal temperatures in terms of N_2 vibrational temperatures. Experiments at CAL were thus conducted on Na-line reversal measurements behind shock waves in N_2 over a similar range of shock temperatures (1720° to 4340° K) by I. R. Hurle[8] to investigate the discrepancy with the earlier line-reversal studies. The results from these further line-reversal measurements in shock-wave flows indicate very good agreement over the entire temperature range with the results of Ref. 15. The discrepancy between the earlier line-reversal results and the results of Ref. 15 was found to be mainly due to inconsistencies in data analysis. The recent line-reversal, shock-wave data[8] show that the Na excitation process has a probability close to unity and proceeds by the near-resonant transfer of vibrational to electronic energy.

This agreement clearly supports the application of line-reversal techniques to the measurement of nozzle-flow vibrational temperatures. It is significant that the rate for N_2 vibrational relaxation behind shock waves is considerably slower at low temperatures than that used in Ref. 1 to calculate the theoretical curves of Fig. 1. The comparisons of Fig. 1 are then somewhat conservative in that the vibrational relaxation times inferred from the nozzle expansion-flow data are even shorter than the value of $1/15\ \tau_s$ indicated. A recalculation of the theoretical curves of Fig. 1 using the more recent correlation for τ_s given in Ref. 8 indicates relaxation times of about $1/70\ \tau_s$ rather than $1/15\ \tau_s$.

Effects of Impurities:

In view of the anomaly between the expansion-flow and shock-wave results for N_2 vibrational relaxation, a brief but systematic study was conducted to determine the nature and extent of the possible effects of typical molecular impurities on the Na line-reversal measurements in N_2 expansion flows[9]. The impurity additives studied were CO_2, O_2, C_2H_2, and H_2O, each being introduced into the initial test gas in the shock tube over a range of initial concentrations from 100 PPM up to about 3000 PPM. The effect of each additive was assessed by the changes which occurred in the line-reversal temperature measurements.

The effect of these additives on the Na line-reversal temperatures in the nozzle expansion flows is shown in Fig. 2 for two reservoir temperatures of T_o = 4250° K and T_o = 3200° K. The two heavy dashes at 100 PPM of additive represent the results of Ref. 1, and the symbols represent the effect of the impurities. The curves are approximations to the experimental data allowing in come cases for the experimental uncertainty of about $\pm$ 30° K. in measured temperature.

The common feature of all the data in this figure is that the additives exert little or no influence on the measured reversal temperatures for initial concentrations less than about 1000 PPM. For higher initial concentrations, the effect of increasing additive, except for O_2 at T_o = 3200° K, is to reduce systematically the measured temperature, i.e., to increase the apparent rate of vibrational relaxation of the N_2.

It is clear from these data that the minimum impurity content which affects the reversal temperature measurements is about one order of

magnitude larger than the estimated impurity content of the N_2 test gas used in the vibrational relaxation studies of Ref. 1. Thus, those results do not appear to be attributable to catalysis of the vibrational relaxation by impurities.

Dilute N_2 Expansions:

Line reversal measurements of vibrational temperature have also been obtained in nozzle expansion flows of a dilute N_2 mixture consisting of 1% N_2 + 99% Ar (Ref. 10). The results of these experiments give N_2 vibrational temperatures consistent with the previous results for 100% N_2. The nitrogen-atom concentration in the dilute-N_2 expansions is considerably smaller than the exceedingly small nitrogen-atom concentration in the 100% N_2 studies. The agreement between the pure and dilute N_2 results, in view of the large differences in nitrogen-atom concentrations, further supports the view[1] that the faster relaxation is not associated with atom-exchange processes of the type proposed by Bauer and Tsang[16]. It may be noted that the dominant collision partners in the 100% N_2 and the dilute N_2 studies are different, being nitrogen molecules and argon atoms, respectively; yet the results are in complete agreement.

Expansion Flow Results of Other Investigators:

Recently other investigators have experimentally studied vibrational relaxation in expansion flows. In particular, Holbeche[13] at the RAE, Farnborough, has used the spectrum-line reversal method to observe N_2 and O_2 vibrational temperatures in a nonsteady expansion flow in a shock tube, while Sebacher[11] at NASA Langley, and Petrie[12] at Ohio State University

have used electron-beam techniques to observe the vibrational temperature of N_2 and air in steady-flow, arc-driven nozzle expansions.

The results of Holbeche for N_2, which were unpublished at the time of writing, are in agreement with those of Ref. 1. Though Holbeche uses a line-reversal technique as in the work of Ref. 1, the nonsteady-flow environment of his experiment is considerably different from the steady expansion-flow environment used at CAL.

Sebacher, on the other hand, has employed the electron-beam technique to measure both the rotational and vibrational temperatures of N_2 in a steady expansion flow. His results also confirm those of Ref. 1. Sebacher's data, including air results, are indicated by the cross-hatched region in Fig. 3. Two theoretical curves are also shown in the Fig. 3. The upper curve gives the theoretical vibrational temperature predicted by the Landau-Teller theory using the most recent correlation[8] of shock-wave data for τ_s, as previously discussed. The lower curve, which fits the experimental data, is the Landau-Teller prediction using the same relaxation time of 1/70 τ_s observed in the re-evaluation of the theoretical curves of Fig. 1. Thus it is seen that the apparent rate of vibrational relaxation in these expansion flows is also about a factor of 70 times faster than in the shock wave flows. It is also interesting to note that the data for air agree well with those for pure nitrogen.

A correlation of all of the available experimental data for vibrational temperatures in expansion flows of N_2 or air can be obtained by dividing the measured vibrational temperatures by the corresponding values predicted by the Landau-Teller theory. In this correlation, shown in Fig. 4, variations

in reservoir pressure and nozzle scale are eliminated. From this figure it is seen that all of the data for N_2 as well as the data of Petrie[12] and Sebacher for air are in good agreement and indicate vibrational temperatures of about 70% of the values predicted on the basis of shock-wave relaxation times.

Thus the results of other investigators confirm the observations of Ref. 1 that vibrational de-excitation of N_2 proceeds much faster in expansion flows than predicted from shock-wave relaxation data, with a consequent reduction in the vibrational temperature.

CO Expansion Flows:

A question of interest is whether N_2 is peculiar in exhibiting this difference between shock-wave and expansion-flow vibrational relaxation, or whether other molecules behave similarly. To investigate the latter possibility, some preliminary experimental studies have been undertaken by A. L. Russo and J. W. Rich to observe the vibrational temperature of CO in nozzle flows using the Na line-reversal technique. The particular choice of CO was primarily based on the availability of extensive relaxation data from the shock-wave studies of Ref. 15. Accordingly, the vibrational relaxation of 5% CO in an argon bath was studied in the nozzle flow for a reservoir pressure of about 45 atm. and reservoir temperatures in the range of about 3600° K to 5200° K.

The vibrational temperatures deduced from these studies at a nozzle area ratio of $A/A^* = 8$ are shown in Fig. 5. The upper curve represents the theoretical temperature predicted by the Landau-Teller theory on the basis of the shock-wave vibrational relaxation times τ_s of Ref. 15. The

lower curves are the Landau Teller predictions for τ = 1/10 and 1/100 τ_s. It is clear from this figure that CO vibration also appears to relax much faster, by almost two orders of magnitude, than expected from previous shock-wave studies. These observations for CO emphasize the inadequacy of present theory for the prediction vibrational relaxation in expansion flows.

O_2 Expansion Flows:

In contradistinction to the N_2 and the present CO measurements, similar Na line-reversal measurements for O_2, done in nozzle expansion flows at CAL by Russo and Hurle and in nonsteady expansion flows at the RAE by Holbeche[17], do not indicate the faster rate of vibrational de-excitation. However, it is felt that the interpretation of these results may be complicated by additional effects. One possible effect is the excitation of Na by resonant energy exchange via low-lying metastable states of O_2. The $a'\Delta_g$ and $b'\Sigma_g^+$ (metastable) states are populated in the equilibrium region behind the reflected shock wave in view of the relatively long residence time. Since these states have very small radiative transition probabilities, it is possible that they also possess relatively small collisional transition probabilities for vibration. Thus these states might remain populated during the expansion flow and thereby be responsible for the apparent excessive Na excitation compared with the results for other gases. This interpretation is consistent with preliminary experiments at CAL which indicate an <u>increase</u> in reversal temperature with increasing O_2 pressure; that is, with increasing number density of O_2 molecules in these metastable states. It is noted that for N_2, the effect of increased N_2 pressure is to <u>decrease</u> the reversal temperature. A second possible effect is associated

with the high reactivity of Na with O_2. It is possible that the Na line-reversal measurements may, in fact, reflect chemical reactions involving Na and O_2.

Theoretical Studies:

Theoretical predictions of vibrational relaxation are generally based on a much simplified model of the inelastic molecular-collision process. These calculations usually neglect molecular rotations, assume a spherically symmetric scattering field, adopt a harmonic oscillator model together with a simplified intermolecular potential, and assume near-adiabatic collisions. It is also customary to use the Landau-Teller transition probabilities where the transition probability for the transfer of a single quantum of vibrational energy is taken to be proportional to the quantum number of the upper state. Recently, a theoretical study has been undertaken at CAL by J. W. Rich to examine the kinetic equations for vibrational relaxation in order to determine how relaxation behavior and level populations are affected when the transition probabilities are not of the Landau-Teller type.

In particular, the following questions have been investigated for a harmonic oscillator model: (1) the conditions under which the mechanism of rapid vibration-vibration exchange insures a Boltzmann distribution, and (2) the effects on vibrational distribution and relaxation of transition probabilities having arbitrary exponential dependence on initial quantum number. Solutions of the master relaxation equation for exponential transition probabilities have been obtained for the two limiting cases of a very dilute mixture

of oscillators in an inert heat bath, and a system consisting only of oscillators. The detailed results of this study are discussed in Refs. 18 and 19.

The results indicate that a Boltzmann distribution among the oscillators is assured, independent of the particular transition probabilities, provided that the resonant (for the harmonic oscillator) vibration-vibration exchange occurs with sufficient frequency. In the case of highly dilute flows this rapid exchange mechanism may not be sufficient to assure a Boltzmann distribution. For the case of extreme dilution, the solution of the master equation for the exponential probabilities shows that the vibrational distribution can differ markedly from a Boltzmann distribution during the relaxation process. For this case, it is found that the upper quantum states tend toward a quasi-equilibrium distribution at early times, and a single relaxation rate cannot be used to characterize the entire relaxation process. However, for a system consisting only of oscillators, where a Boltzmann distribution is assured by the vibration-vibration exchange mechanism, the solution obtained for exponential transition probabilities does not differ significantly from the Landau-Teller result.

Effects of anharmonicity are clearly of interest and are currently being investigated.

3. NONEQUILIBRIUM EFFECTS ON WEDGE-FLAT PLATE AFTERBODY PRESSURES*

The second study to be reviewed concerns shock tunnel experiments with air at high total enthalpies to determine nonequilibrium effects on the surface pressure of a flat plate with a wedge leading edge. This study was carried out by R. J. Vidal and F. Stoddard; a comprehensive account is given in Ref. 2.

Nonequilibrium effects in external flows of this kind have been of interest for many years because of their possible importance on the aerodynamic characteristics of flight vehicles at high velocities. Despite this interest, however, very few experiments have been done which demonstrate even such gross nonequilibrium effects as those on model surface pressure. Most of our knowledge of such effects comes from calculations; wind tunnel experiments in this area are difficult to do for several reasons. Although nonequilibrium flow-field calculations are most invaluable and necessary, at least a minimum level of experimentation is obviously desirable. Even an overall experimental check on gross effects, such as on pressure, would appear to be worthwhile in view of the various uncertainties in thermochemical kinetic models and rate constants for air. The present study was undertaken from this point of view.

Model Test Flow Conditions

The simple wedge-plate geometry of the model was chosen because it is representative of elements of more complex flight configurations, and because the corresponding nonequilibrium flow is relatively easily analyzed,

*This work was sponsored jointly by the Arnold Engineering and Development Center under Contract No. AF 49(600)-928, and by the NASA, Langley Research Center, under Contract NAS 1-2812.

at least in approximate fashion adequate for the present objective. Apart from providing a direct comparison of nonequilibrium-flow theory with experiment, analysis of the flow was necessary in order to obtain an equilibrium-flow reference result, as is usually the case with experiments of this type.

The model, shown in Fig. 6, consisted of a 42.5°-wedge leading-edge flat plate instrumented for surface pressure measurement with piezoelectric transducers and for surface heat-transfer measurement with thin-film resistance thermometers. The wedge angle was chosen to produce a strong shock wave which would be attached under both ideal (frozen) and equilibrium air conditions. Two model thicknesses, 1/2 and 4 inches, were used in order to vary the level of excitation of internal degrees of molecular freedom (vibration and dissociation) attained in the wedge flow field before rapid Prandtl-Meyer expansion occurred around the wedge-plate corner. With the 1/2-inch thick model, the experimental flow fields were essentially frozen throughout, whereas with the 4-inch thick model, significant vibrational excitation and dissociation were produced in the wedge shock-layer before the flow expanded around the wedge-plate corner.

Tests were conducted with both small and large-scale models in the CAL 4-foot and 6-foot hypersonic shock tunnels described in Refs. 20 and 21, respectively. A detailed summary of test conditions is shown in Table I. The tunnel reservoir temperatures for these tests were about 3200° K in the 4-ft. tunnel and 6250 to 6650° K in the 6-ft. tunnel. Chemical nonequilibrium effects in the ambient test flow at the higher reservoir temperatures were determined by calculation using the CAL computer program

for nonequilibrium nozzle expansions[22, 23] in conjunction with measured pitot pressures. The computer program assumes vibrational equilibrium of the diatomic air species, but a general, coupled-reaction model for chemical nonequilibrium.

Viscous effects played a significant role in all of the experiments. For this reason, surface heat-transfer distributions as well as surface pressures were measured on the flat plate. In the small-scale model experiments, the model flow field was essentially frozen, or that of an ideal gas, at both low and high reservoir temperatures. The interest here was in extending the correlation of viscous interaction/bluntness effects under ideal-gas conditions to higher temperature flow fields than previously studied.

In the large-scale model experiments, the conditions for the high-temperature tests were chosen to produce maximum dissociation in the wedge flow field within the limits of the prevailing performance of the 6-foot shock tunnel (which have since been extended). However, in spite of maximizing the real gas effects, severe boundary layer thickening in the corner expansion and flat-plate afterbody flow produced viscous interaction effects on the pressure which were comparable to the nonequilibrium effects of interest. Thus, careful attention was required of the boundary layer influence in order to interpret the real gas behavior. The low-temperature experiments with the large-scale model were carried out primarily to assess the boundary layer influence.

Calculation of Inviscid Afterbody Pressure on the Large-Scale Model

Approximate theoretical analysis of the inviscid nonequilibrium flow field was done for the large-scale model to obtain a prediction of the inviscid flat-plate pressures for comparison with experiment. Basically, the approach was to calculate the thermochemical nonequilibrium aspects of the wedge flow field by neglecting curvature of the wedge shock wave and streamlines, as well as pressure and velocity variations along streamlines, induced by nonequilibrium. In particular, the thermochemical behavior along the wedge surface was computed using a machine program for nonequilibrium normal shock-wave airflows previously developed at CAL[24]. For the Prandtl-Meyer corner expansion, various estimates indicated that very rapid freezing would occur at the conditions of interest, particularly for streamlines near the corner. Thus, a first approximation to the initial flat-plate inviscid pressure was obtained by assuming a completely frozen expansion from the nonequilibrium state calculated as above for the wedge surface streamtube.

The chemical-kinetic air model for these calculations was essentially that shown for the neutral species in Table II and included the usual dissociation-recombination reactions for O_2, N_2, and NO as well as the bimolecular "shuffle" reactions $N + O_2 \rightleftharpoons NO + O$ and $O + N_2 \rightleftharpoons NO + N$. Vibration was important as an energy sink in the wedge flow field in both the low and high-temperature experiments. Two different vibrational models were employed to obtain some assessment of the effects of vibrational relaxation. In one model, complete vibrational equilibrium of all diatomic species was assumed. In the other, N_2 and O_2 were allowed to

relax independently in vibration at the individual rates determined by Blackman[14], uncoupled from dissociation, while NO was completely equilibrated in vibration. The assumption of vibrational equilibrium for NO rested on extrapolation of Wray's data[25] to the wedge flow field conditions. This gave a relaxation length for NO vibration very much smaller than the wedge length, whereas the relaxation lengths for O_2 and N_2 vibration were, respectively, of the same order as or much greater than the wedge length. Of course, these vibrational models are relatively crude, but they give some indication of the possible limiting effects of vibrational relaxation. It is recognized that for air, various coupling mechanisms such as vibration-vibration exchange could play a role. Detailed consideration of such effects, which are not well understood, was outside the scope of the present study. Corrections for source-flow effects were made to the calculated inviscid-flow pressures (following Ref. 26) in order to permit a comparison of theory with the experimental data obtained in the conical nozzles of the shock tunnels.

Experimental Results

The discussion of the results of this study is confined to the large-scale model experiments where significant thermochemical excitation occurred in the wedge flow field. The results for the small-scale model tests, including an extended correlation developed for heat-transfer and pressure distributions, are discussed in detail in Ref. 2.

Surface pressure, surface heat transfer, and schlieren observations for the low-temperature experiments, are shown in Figs. 7, 8, and 9, respectively. These data were obtained from tests with the large-scale

model in the CAL 4-ft. shock tunnel at a reservoir temperature of 3290° K and a reservoir pressure of 260 atm.

Several features of these low-temperature results may be noted. First, the surface pressure (Fig. 7) shows a decrease by about a factor of 2 downstream of the wedge-plate corner. This is unlike the inviscid, ideal-gas flow behavior whereby the pressure should be constant to $x/t \approx 3.2$, after which the expansion-fan characteristics reflected from the shock wave strike the body. In contrast to the pressure, the heat transfer (Fig. 8) shows approximately the variation expected from thin boundary layer considerations. A second feature is the apparent very thick boundary layer on the flat-plate afterbody indicated in the schlieren photograph of Fig. 9, which increases in thickness slowly with increasing distance downstream. The wedge boundary-layer thickness at the corner is only about 1/10 that on the afterbody. A third feature to be noted is the apparent secondary shock wave in the afterbody flow field of Fig. 9.

The pressure decay downstream of the corner is interpreted by Vidal and Stoddard[2] as a boundary-layer displacement effect. This interpretation is strongly supported by the schlieren evidence of a thick boundary layer and by the theoretical considerations in Ref. 2 of the behavior of a boundary layer under the influence of such a strong corner expansion. On the basis of assumed local similarity, the variations of pressure, heat transfer, and boundary-layer displacement thickness observed in the experiments are shown to be closely predicted by boundary layer theory. This is evident in Figs. 7, 8, and 9 where theoretical variations based on local similarity are included. Regarding the formation of the secondary shock

wave evident in Fig. 9, this is shown to be plausible in Ref. 2 on the basis of a momentum-integral approach to the behavior of the boundary-layer displacement thickness, an approach which generalizes earlier work by Stroud[27]. The analysis of Ref. 2 strongly suggests that a locally compressive flow will be produced by rapid boundary layer thickening on flow expansion around such a convex corner.

Figure 7 shows several calculated values for the flat-plate pressure (labelled asymptotic plate pressures) based on inviscid flow and the various assumptions indicated for vibrational excitation. One might expect these "inviscid" pressure levels to be approached after the initial large displacement effects have diminished. Under the conditions of these low-temperature experiments, molecular dissociation was unimportant. On the basis of the relaxation lengths of pure O_2 and N_2, the assumption of vibrationally equilibrated O_2 but vibrationally frozen N_2 is reasonable for the upstream point of the wedge-plate corner. This assumption, coupled with that of a vibrationally-frozen corner expansion, gives a pressure level (labelled 5 in Fig. 7) in fair agreement with the most downstream experimental data points. This level is about twice as great as that produced by a frozen expansion from an initial state of complete equilibrium (labelled 6).

The assumption of a frozen corner expansion appears reasonable on the basis of estimates which indicate complete vibrational freezing within the initial 5 to 10° of the Prandtl-Meyer expansion. For the inviscid flat-plate afterbody flow, the vibrational relaxation length for recovery to equilibrium is estimated as in excess of 200 feet.

Typical high-temperature test results for pressure distribution, corresponding to those of Fig. 7, are shown in Fig. 10 for a nozzle reservoir temperature of 6650° K and a reservoir pressure of 1140 atm. At these conditions, in addition to vibrational excitation, appreciable dissociation of O_2 was predicted to occur along the wedge surface streamtube prior to flow expansion around the corner.

The pressure decay downstream of the corner is interpreted as a boundary layer displacement effect as discussed above. In Ref. 2, consideration is given to several inviscid effects which could cause a variation in the afterbody surface pressure. In particular, the variation of flow properties along the leading characteristic of the expansion fan is estimated to have only small influence in this respect. It will be noted in Fig. 10 that there is a marked levelling off in the pressure; this behavior is typical of all the high temperature tests. The dashed curve is the initial variation in pressure predicted on the basis of a locally similar boundary layer.

The various theoretical pressure levels shown in Fig. 10 are the inviscid-flow estimates discussed above for the surface streamtube under the assumptions indicated as regards vibration and dissociation. Source-flow corrections are included. The experimental pressure data appear to level off between the calculated limits for equilibrium and nonequilibrium vibration in the wedge flow field, assuming finite-rate chemistry and a frozen expansion at the corner in both cases.

In conclusion regarding this study, the afterbody pressure data obtained for the large-scale model are interpreted as showing substantial effects of thermochemical nonequilibrium in the flow field. Typically, the

final afterbody pressures lie 40% below ideal-air values and 25 to 35% below equilibrium-air values. Although the interpretation is complicated by substantial boundary-layer effects, the final pressure levels attained agree fairly well with the inviscid-flow estimates. However, because of the boundary layer effects and the general complexity of the thermochemistry, more definitive conclusions cannot be drawn regarding the correctness of the particular vibration-dissociation models assumed.

4. CALCULATION OF THE NONEQUILIBRIUM PLASMA SHEATH ABOUT BLUNT RE-ENTRY BODIES AT ANGLE OF ATTACK*

The third study to be discussed concerns calculation of nonequilibrium inviscid flow fields about blunt axisymmetric bodies at arbitrary angle of attack. The direct motivation of this work is the need to determine the bounds of radio communication blackout during earth re-entry of space vehicles, with particular emphasis on Apollo re-entry. Communication blackout results from the presence of free electrons in the re-entry body flow field or plasma sheath through which the electromagnetic signal must be transmitted. Thus the electron density, as well as the electron collision frequency, are quantities of primary interest throughout most of the plasma sheath. Given the distribution of these quantities, the attenuation of electromagnetic propagation can be estimated.

The calculation of the electron density distribution in any exact sense is a very difficult undertaking. Even for an ideal gas, the fluid dynamic

*This work was sponsored by NASA, Goddard Space Flight Center, under Contract NAS 5-3976.

problem is formidable since, in general, blunt forebodies at angle of attack are involved. Further, Apollo-type re-entry shapes have a re-entrant conical afterbody which promotes flow separation. In addition to the basic fluid dynamic problem, the second major problem is, of course, the chemical kinetics of ionized air. At velocities around 36,000 ft/sec, appropriate to Apollo re-entry, a number of ionization mechanisms appear to be important. A large number of ionization reactions must therefore be considered. For many of these reactions, the rate constants are not well known.

The work discussed herein is concerned primarily with calculation of the inviscid flow over an Apollo-type forebody at angle of attack. This work is part of a larger research program at CAL on the Apollo plasma sheath which includes analysis of the corresponding afterbody flow and associated viscous phenomena, as well as experimental study of the pertinent ionization reactions.

Basic Method of Calculation

The basic method of calculation, which has been developed and described by Bohachevsky and Mates[3,4], is a time-dependent direct method suitable for machine computation. In this method the time derivatives are retained in the governing differential (Euler) equations which thereby are always hyperbolic. The solution to a given steady-flow problem is then obtained as the asymptotic numerical solution for large times to a corresponding initial-boundary value problem in nonsteady flow. In particular, in the present applications to blunt body flows the body is impulsively accelerated from rest to a constant velocity at time zero. The consequent transient

flow field is calculated forward in time until it no longer changes. The particular numerical method used is a generalization of a scheme first proposed by Lax[33] which allows flow field discontinuities such as shock waves to be accommodated. Several powerful advantages characterize the method. It is direct, in contrast to inverse methods where the shock wave shape must be specified a priori, it is applicable to arbitrary angles of attack, avoids the difficulty of unknown boundary conditions, and does not require iterative procedures. The penalty for these advantages is the increase by one in the number of independent variables.

This nonsteady-flow direct method has been programmed for the IBM-7044 computer, and a number of specific examples of blunt body flows have been computed for the simplified case of an ideal gas. Recently, the basic program has been extended to include an arbitrarily general gas model describing the chemical kinetics of the nonequilibrium flow field. Application of the method to three-dimensional flows is complicated by the large number of space-time computational mesh points involved, which necessitates a large data storage capacity. With the available IBM 7044 computer, the use of magnetic tapes for auxiliary data storage has therefore been necessary. The use of magnetic-tape storage does not greatly increase the computing time since random access recovery is not used with the tapes.

As a basis for obtaining the interim estimates of the nonequilibrium electron density field to be discussed below, the above method has been applied to calculate the ideal-gas flow field about an Apollo-shaped vehicle at an angle of attack of 20° and a free stream Mach number of 28.9. This Mach number corresponds to a velocity of 30,000 ft/sec at a altitude of

200,000 ft. in the 1959 ARDC atmosphere. The calculated shock shape and streamline pattern, as well as the body shape, for the plane of symmetry of this flow field are shown in Fig. 11. The body is axisymmetric and consists of a re-entrant conical afterbody of 70° total cone angle, with a spherical forebody cap. The small circles in Fig. 11 define the shock shape predicted by the empirical correlation of Kaattari[28].

Detailed discussion of the results for this case, as well as for the axisymmetric-flow case, is given by Bohachevsky and Mates[4]. In general, the results agree well with the limited amount of other data that are available for comparison. The stagnation point for the 20° angle-of-attack case of Fig. 11 is found to be located at an angular position of 15° to the body axis. This may be compared to an experimental value of 14.5° deduced from Ref. 28. It is evident from Fig. 11 that the calculated shock shape also agrees well with the experimentally-based correlation of Ref. 28. Good agreement is found in recently made comparisons of predicted and experimental pressure distributions. As expected, the forebody pressure distribution is roughly Newtonian. One further feature of the solution worth noting is that the maximum entropy streamline, which crosses the shock wave normally, does not wet the body surface.

Application to Nonequilibrium Plasma Sheath

In order to obtain interim estimates of Apollo plasma-sheath ionization, the above solution for the ideal-gas flow field at 20° angle of attack has been used as a basis for further calculations to determine nonequilibrium ionization along a number of selected streamlines in the plane of symmetry of the flow. These calculations have been carried out by Dunn et al[5] for the

body of Fig. 11 with a spherical-cap radius of 15.5 ft., a velocity of 30,000 ft/sec, and for altitudes of 200 and 250 k ft. The basic approach was to use the streamline pressure distributions from the ideal-gas solution as the boundary condition or input data for machine calculation of the individual streamline thermochemical behavior. The latter calculation was done with a machine program previously developed at CAL[22, 23] for inviscid streamtube or nozzle flows with arbitrary coupled chemistry.

The chemical kinetic model for ionized air used for these calculations is a further development of that first used by Eschenroeder et al[29]. The model is discussed in some detail in Ref. 5, and a comprehensive review of the rate constants has recently been made by Dunn[30]. A basic assumption of the model is that molecular rotation and vibration as well as the energies of bound and free electrons are equilibrated with the translational energy. Tables II and III from Ref. 5 show the chemical reactions and rate data employed for the neutral and ionized species, respectively (the reverse reactions were also included in the calculations).

In the re-entry velocity range of interest, both the neutral and ionized species can be important as regards the flow thermodynamics and must, in general, be calculated simultaneously. As is evident from Table III, the ionization kinetics of air are quite complex and require consideration of a large number of individual reactions. Apart from obtaining estimates of electron density, an important purpose of these calculations was to determine which of the ionization reactions were unimportant and could be eliminated in order to simplify the ionization kinetic model. Important classes of reactions include the two-body processes of impact ionization,

dissociative recombination, charge exchange, and ion-atom exchange, and the three-body process of electron recombination. In general, the rate constants for the ionization reactions are much more uncertain than those for the neutral species chemistry. Estimates by M. G. Dunn at CAL show that these uncertainties in rate constants can significantly influence the electron density in Apollo-type plasma flows. One of the largest uncertainties exists for the three-body process of electron-electron-ion recombination. This reaction, and the two-body reverse process of impact ionization, is a dominant reaction in the Apollo plasma.

Streamtube Results

Detailed discussion of the results of the above streamtube calculations for the Apollo-type flow field is given in Ref. 5 and only the broader features of the results will be summarized here. As expected, the nonequilibrium behavior of the flow field exhibits certain basic features determined by the particular gasdynamic environment of a blunt-body shock layer. In general, after streamlines cross the bow shock wave their chemistry tends to look initially like that behind a normal shock wave of appropriate strength. This initial behavior is then modified by the subsequent flow expansion around the body. The strong expansion beginning at, and downstream of, the sonic line generally tends to reduce drastically the rates of chemical reaction. In general, the calculated flow-field chemistry and ionization is found to be far from equilibrium. Fluid particles crossing the bow shock wave where it is strongest, i.e., in the vicinity of the stagnation streamline, experience the largest increase in static enthalpy and thereby the largest amount of dissociation and ionization. Static enthalpies decrease rather

strongly with decreasing bow-shock angle, and away from the stagnation streamline there is consequently a tendency towards frozen flow. This tendency is further promoted by the associated higher fluid velocities and smaller residence times in the outer regions of the field.

At the velocities considered, extensive dissociation of N_2 and O_2 occurs along the higher enthalpy streamlines (the dissociation of O_2 is essentially complete). As observed in previous studies[31], the mass concentrations of neutral nitrogen and oxygen atoms tend strongly to freeze at high levels in the ensuing gasdynamic expansion around the body. Regarding the charged particles, free electrons, of course, are the dominant of the individual charged species. Close to the bow shock, molecular ions are the dominant ions, N_2^+, O_2^+, and NO^+ all being initially important on the high enthalpy streamlines. On the lower enthalpy streamlines, only NO^+ is initially important. Following the initial post-shock region of molecular ionization, atomic ionization (N^+ and O^+) becomes important, particularly at higher enthalpies. In contrast to the behavior of the neutral atoms, the charged species show little tendency to freeze in the flow expansion around the body. This is a consequence of both two-body dissociative-recombination, which is relatively fast at low densities, and the fast three-body recombination of electrons where free electrons serve as third bodies.

Analysis of the contributions of individual reactions shows that little general simplification of the ionization model is possible by eliminating reactions. Almost all of the reactions considered become important in some part of the flow field. Thus, the only significant simplifications possible would be limited to specific regions of the flow field.

As mentioned previously, the flow field chemistry and ionization is generally far from equilibrium. Figure 12 shows contours of constant electron density (electrons/cm^3) in the plane of symmetry deduced from the calculations for the case of 200 k ft. altitude. The maximum electron density occurs in the vicinity of the stagnation point and is about 5×10^{15} electrons/cm^3. This density falls to about 10^{14} at the windward and leeward corners of the body. Corresponding plots have also been made for electron-neutral and electron-ion collision frequencies[5]. The maximum total collision frequency is of the order of 10^9 to 10^{10}/sec. For 250 k ft. altitude, electron densities are roughly 50 times less and total collision frequencies about 10 times less.

For the purpose of estimating electromagnetic wave attenuation, electron densities and collision frequencies were determined along the two paths labelled A and B (Fig. 12) emanating from the body slightly downstream of the windward and leeward corners, respectively. A surprising feature of this determination is that the electron density does not vary strongly and remains relatively high along both paths from body to shock wave. The density exceeds 10^{14} electrons/cm^3 for most of path A and 2×10^{13} for most of path B. Total collision frequencies along both paths likewise do not vary strongly, being in the vicinity of 10^9/sec. These results are for 200 k ft. altitude. The high electron densities prevailing over most of the paths considered emphasize the importance of the inviscid outer flow field for electromagnetic wave attenuation.

The total attenuation of plane electromagnetic waves along these two paths, calculated by a technique suggested by Bein[32], is shown in Fig. 13.

This calculation is based on the assumption that gradients normal to the propagation path are small, an assumption which is not well satisfied in the present example. However, the results obtained should at least be representative. As evident from Fig. 13, the predicted attenuation is severe for both paths, being in excess of 100 db for frequencies below a few hundred gigacycles/sec.

5. CONCLUDING REMARKS

This paper has reviewed three studies of nonequilibrium flows which have been carried out in the Aerodynamic Research Department of the Cornell Aeronautical Laboratory. These investigations constitute part of a broad continuing program at CAL on nonequilibrium-flow research. On two of the studies described, namely, on vibration relaxation phenomena and on Apollo plasma-sheath nonequilibrium, additional research is currently underway. On the wedge flat-plate flow, which is not presently being studied further, additional investigation of the boundary layer behavior, solely from the fluid dynamic viewpoint, would appear to be worthwhile.

REFERENCES

1. Hurle, I. R., Russo, A. L., and Hall, J. G., J. Chem. Phys., 40, 2076 (1964)
2. Vidal, R. J. and Stoddard, F., NASA Contractor Report CR-328 (Nov. 1965). Also, CAL Report AF-1817-A-1 (May 1965)
3. Bohachevsky, I. O. and Mates, R. E., AIAA Paper 65-24 (Jan. 1965)
4. Bohachevsky, I. O. and Mates, R. E., CAL Report AI-1972-A-4 (Dec. 1965)
5. Dunn, M. G., Daiber, J. W., Lordi, J. A., and Mates, R. E., CAL Report AI-1972-A-1 (Sept. 1965)
6. Gaydon, A. G. and Hurle, I. R., The Shock Tube in High Temperature Chemical Physics. Chapman and Hall, Ltd., London, and Reinhold Publishing Corp., N. Y. 1963
7. Russo, A. L., Hall, J. G., and Lordi, J. A., CAL Report AD-1689-A-4 (1964)
8. Hurle, I. R., J. Chem. Phys., 41, 3911 (1964)
9. Russo, A. L., J. Chem. Phys., 44, 1305 (1966)
10. Hurle, I. R. and Russo, A. L., J. Chem. Phys., 43, 4434 (1965)
11. Sebacher, D. I., Private communication on work to be published
12. Petrie, Stuart L., Proceedings of the 1965 Heat Transfer and Fluid Mechanics Institute, Stanford University Press, 1965
13. Holbeche, T. A., Private Communication
14. Blackman, J., J. Fluid Mech., 1, 61 (1956)
15. Millikan, R. C. and White, D. R., J. Chem. Phys., 39, 98 (1963)
16. Bauer, S. H. and Tsang, S. C., Phys. Fluids, 6, 182 (1963)
17. Holbeche, T. A., Nature, 203, 476 (1964)
18. Rich, J. W. and Rehm, R. G., 11th International Symposium on Combustion, Berkeley, Calif., Aug. 14-20, 1966 (To be published)

19. Rich, J. W., American Physical Society Division of Fluid Dynamics Annual Meeting, Paper B-7, Cleveland, Ohio, Nov. 22-24, 1965

20. Experimental Facilities Division Hypersonic Shock Tunnel, Description and Capabilities. CAL Report (Oct. 1964)

21. Hilton, J., Fabian, G. J., Golian, T. C., Wilson, M. R., and Somers, L., Development and Performance of the CAL Six-Foot Shock Tunnel. (CAL Report to be issued)

22. Eschenroeder, A. Q., Boyer, D. W., and Hall, J. G., Phys. Fluids, 5, 615-624 (1962)

23. Lordi, J. A. and Mates, R. E., CAL Report AD-1689-A-6 (Oct. 1965)

24. Marrone, P. V., CAL Report QM-1626-A-12(I) (May 1963)

25. Wray, K. L., AVCO Research Report 96 (June 1961)

26. Hall, J. G., CAL Report 128 (Aug. 1963)

27. Stroud, J., ARS J., 664-665 (May 1961)

28. Kaattari, G. E., NASA TN D-1980 (Dec. 1963)

29. Eschenroeder, A. Q., Daiber, J. W., Golian, T. C., and Hertzberg, A., CAL Report AF-1500-A-1 (July 1962)

30. Dunn, M. G., Reaction Rate Constants for Charged Species in Air. (CAL Report to be issued)

31. Hall, J. G., Eschenroeder, A. Q., and Marrone, P. V., J. Aerospace Sci., 29, 1038-1051 (Sept. 1962)

32. Bein, G. P., AIAA Paper No. 66-173 (March 1966)

33. Lax, P. D., Communs. Pure and Appl. Math., 7, 159-193 (1954)

TABLE I SUMMARY OF TEST CONDITIONS

Test Identification	Facility	Reservoir Conditions		Ambient Conditions at the Model Station			
		Temperature °K	Pressure psia	Density Ratio ρ/ρ_{SL}	Velocity Ft/Sec	Mach Number	Reynolds Number/in
Large Scale Model							
High Temp. No. 1	6-ft. Shock Tunnel	6650	16,700	2.28×10^{-4}	14,900	16.3	2680
High Temp. No. 2	6-ft. Shock Tunnel	6200	9,900	5.50×10^{-4}	14,580	12.0	3940
High Temp. No. 3	6-ft. Shock Tunnel	6250	11,050	2.47×10^{-4}	14,750	14.3	2320
Low Temperature	4-ft. Shock Tunnel	3290	3,820	6.01×10^{-4}	9,370	15.0	9210
Small Scale Model							
High Temperature	6-ft. Shock Tunnel	6570	15,620	5.26×10^{-5}	14,800	22.4	1082
Low Temperature	4-ft. Shock Tunnel	3180	750	5.75×10^{-5}	9,210	17.5	1216

TABLE II
AIR REACTIONS FOR NEUTRAL SPECIES

$k_{F_i} = A_i T^{n_i} \exp(-\theta_i/T)$, cc/mole sec for T in °K

SPECIES CONSIDERED ARE: N_2, O_2, NO, N, O, Ar

REACTION	COLLISION PARTNER, M	A_i	n_i	θ_i
$N_2 + M \xrightarrow{k_{F_i}} 2N + M$	N_2	3.0×10^{21}	-1.5	113260
$N_2 + M \longrightarrow 2N + M$	N	1.5×10^{22}	-1.5	113260
$N_2 + M \longrightarrow 2N + M$	Ar, O, O_2, NO	9.9×10^{20}	-1.5	113260
$O_2 + M \longrightarrow 2O + M$	O_2	3.6×10^{21}	-1.5	59380
$O_2 + M \longrightarrow 2O + M$	O	2.1×10^{18}	-0.5	59380
$O_2 + M \longrightarrow 2O + M$	Ar, N, N_2, NO	1.2×10^{21}	-1.5	59380
$NO + M \longrightarrow N + O + M$	Ar, N_2, O_2, N, O	5.2×10^{21}	-1.5	75490
$N + O_2 \longrightarrow NO + N$		1.0×10^{12}	0.5	3120
$O + N_2 \longrightarrow NO + N$		5.0×10^{13}	0	38000
$NO + NO \longrightarrow N_2 + O_2$		4.8×10^{23}	-2.5	43000

TABLE III
AIR REACTIONS FOR IONIZED SPECIES

$k_{F_i} = A_i T^{n_i}$ $cm^3/mole\ sec$ (2 body reactions)

$k_{F_i} = A_i T^{n_i}$ $cm^6/mole^2\ sec$ (3 body reactions)

for T in °K

SPECIES CONSIDERED ARE: N_2^+, O_2^+, NO^+, N^+, O^+, and e^-

REACTION	M	A_i	n_i
DISSOCIATIVE RECOMBINATION REACTIONS			
$e^- + NO^+ \longrightarrow N + O$		1.8×10^{21}	-1.5
$e^- + N_2^+ \longrightarrow N + N$		1.0×10^{21}	-1.5
$e^- + O_2^+ \longrightarrow O + O$		1.0×10^{21}	-1.5
THREE-BODY RECOMBINATION REACTIONS			
$e^- + NO + NO^+ \longrightarrow N_2 + O_2$		1.0×10^{24}	-2.5
$e^- + N + M^+ \longrightarrow N + M$	NO, N, O, O_2, N_2	6.0×10^{24}	-2.5
$e^- + O + M^+ \longrightarrow O + M$		6.0×10^{24}	-2.5
$e^- + N_2 + M^+ \longrightarrow N_2 + M$		2.22×10^{26}	-2.5
$e^- + O_2 + M^+ \longrightarrow O_2 + M$		8.8×10^{26}	-2.5
$e^- + NO + M^+ \longrightarrow NO + M$		1.31×10^{28}	-2.5
$e^- + e^- + M^+ \longrightarrow e^- + M$		8.3×10^{39}	-4.5
CHARGE-EXCHANGE REACTIONS			
$O + M^+ \longrightarrow M + O^+$	N, N_2	7.8×10^{11}	0.5
$N + N_2^+ \longrightarrow N_2 + N^+$			
$O_2 + M^+ \longrightarrow M + O_2^+$	O, N, N_2		
$NO + M^+ \longrightarrow M + NO^+$	O, N, O_2, N_2		
ION-ATOM EXCHANGE REACTIONS			
$O + N_2^+ \longrightarrow N + NO^+$		7.8×10^{11}	0.5
$N + O_2^+ \longrightarrow O + NO^+$			
$N_2 + O^+ \longrightarrow N + NO^+$			
$N_2 + O_2^+ \longrightarrow NO + NO^+$			
$O_2 + N^+ \longrightarrow NO + O^+$			
$O_2 + N^+ \longrightarrow O + NO^+$			
$O_2 + N_2^+ \longrightarrow NO + NO^+$			
$NO + O^+ \longrightarrow N + O_2^+$			
$NO + N^+ \longrightarrow O + N_2^+$			
$NO + N^+ \longrightarrow N_2 + O^+$			

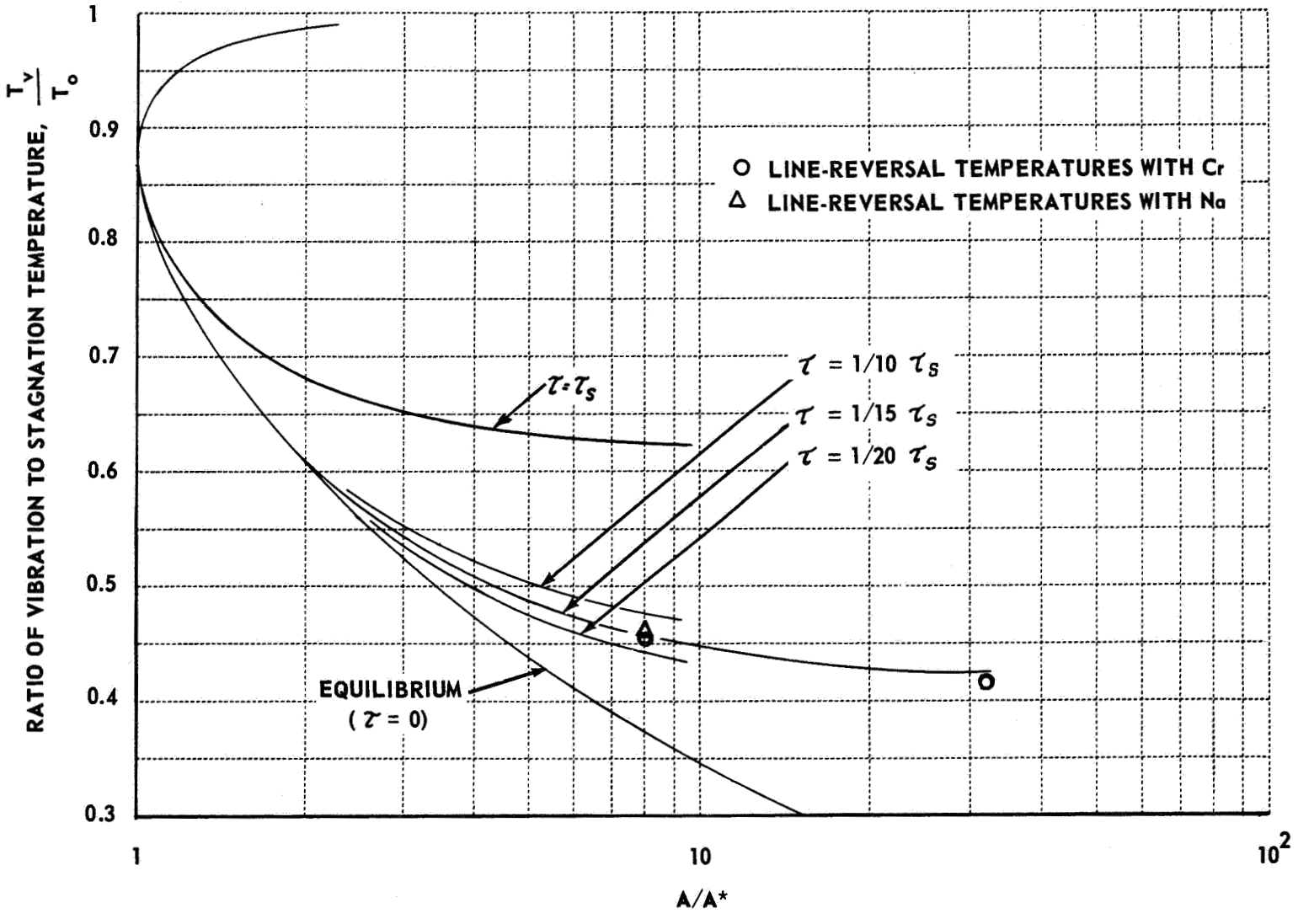

Figure 1 COMPARISON OF TYPICAL MEASURED VIBRATIONAL TEMPERATURES WITH THEORY FOR N_2 EXPANSIONS IN 15° CONICAL NOZZLE.
T_o = 4500 °K, P_o = 50 ATM

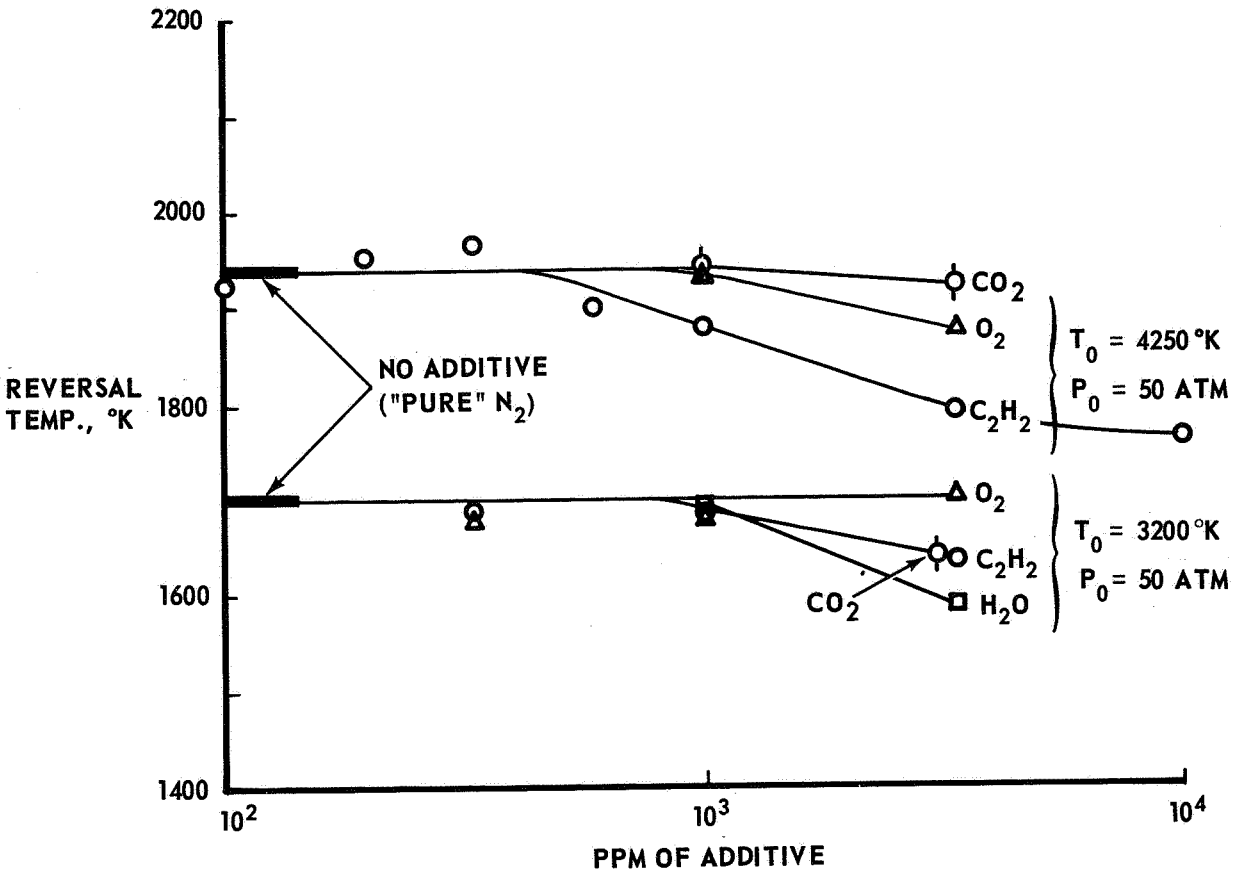

Figure 2 EFFECT OF ADDITIVES ON MEASURED LINE-REVERSAL TEMPERATURES IN N_2 EXPANSIONS

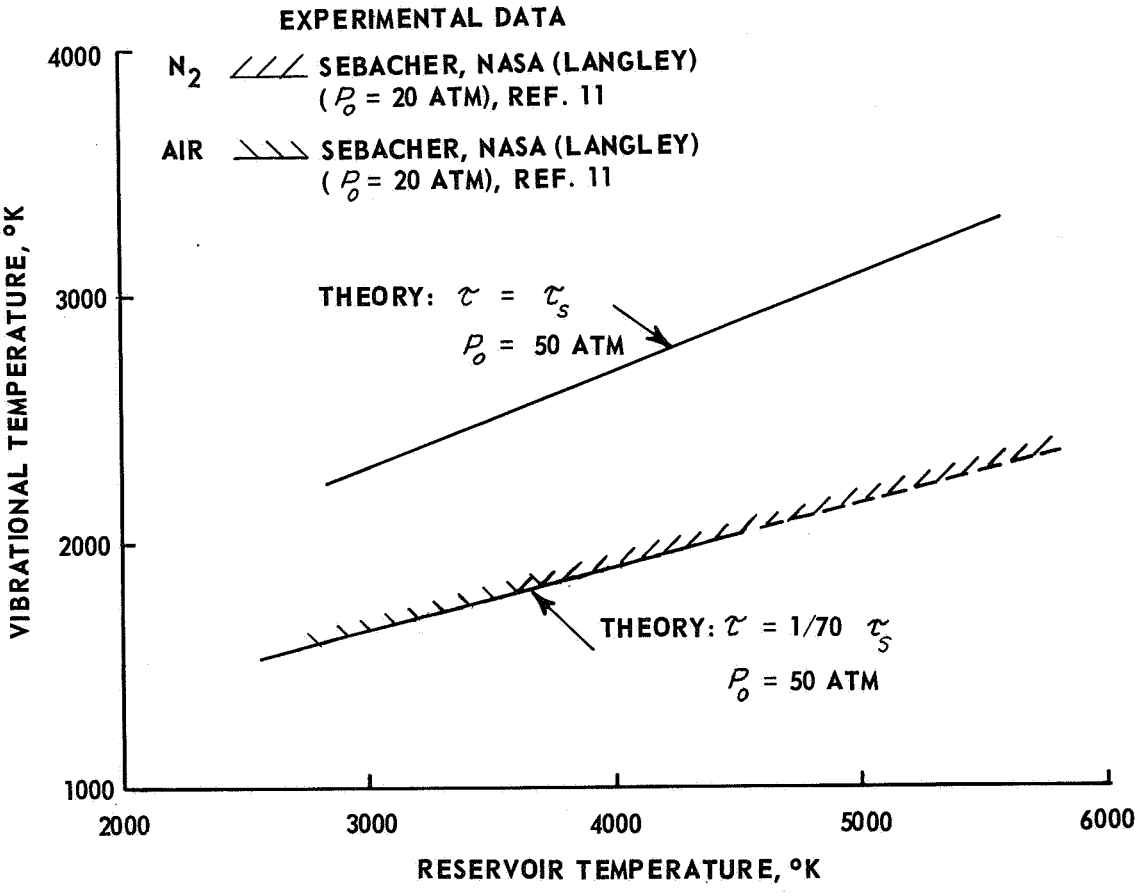

Figure 3 VIBRATIONAL RELAXATION OF N_2 AND AIR IN NOZZLE EXPANSION FLOWS

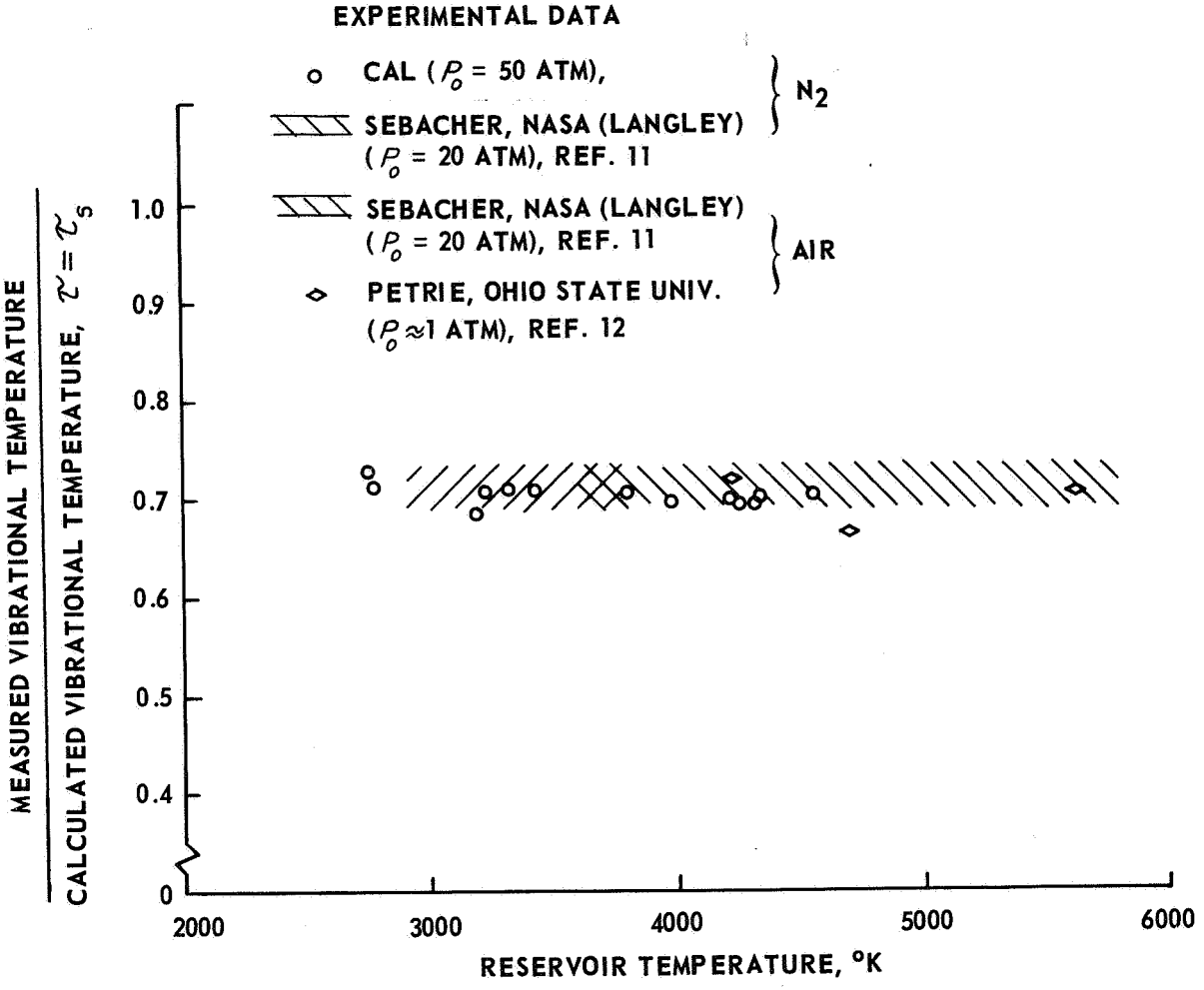

Figure 4 NORMALIZED VIBRATIONAL TEMPERATURES OF N_2 AND AIR IN NOZZLE EXPANSION FLOWS

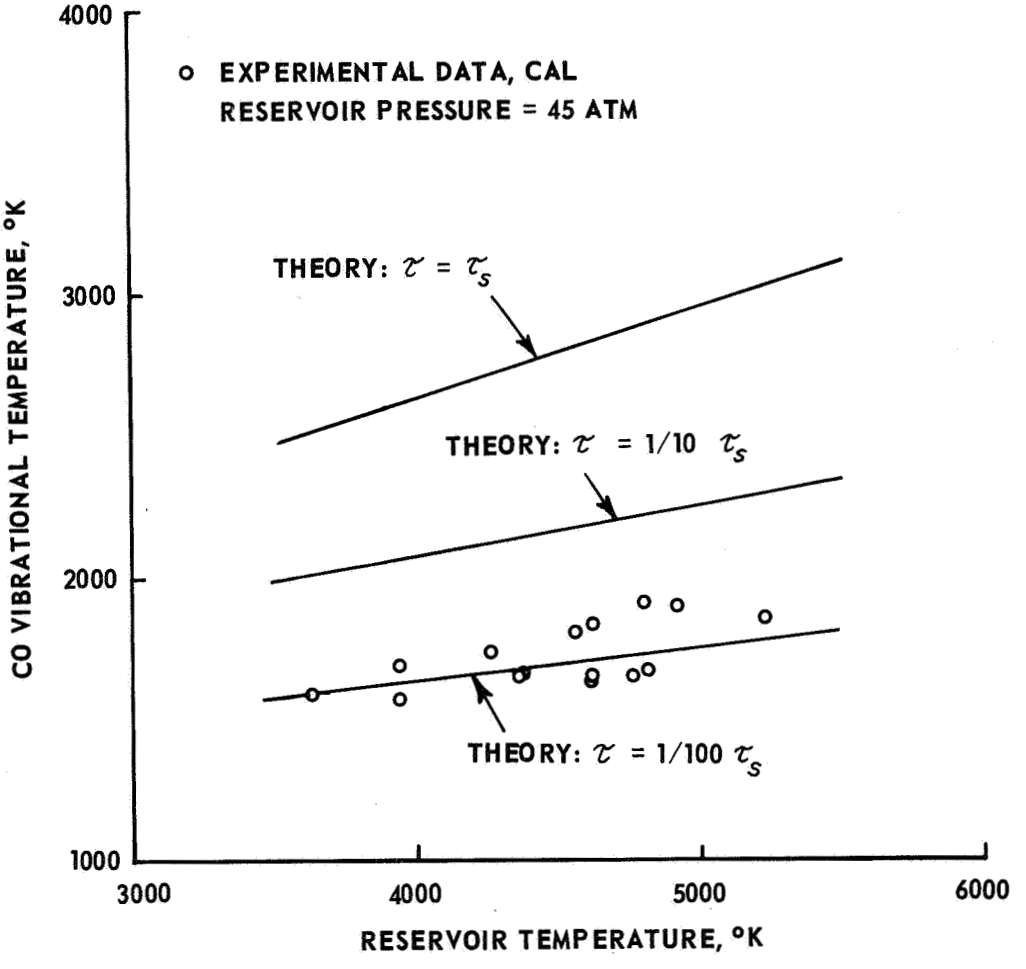

Figure 5 VIBRATIONAL RELAXATION OF 5% CO IN ARGON IN NOZZLE EXPANSION FLOWS

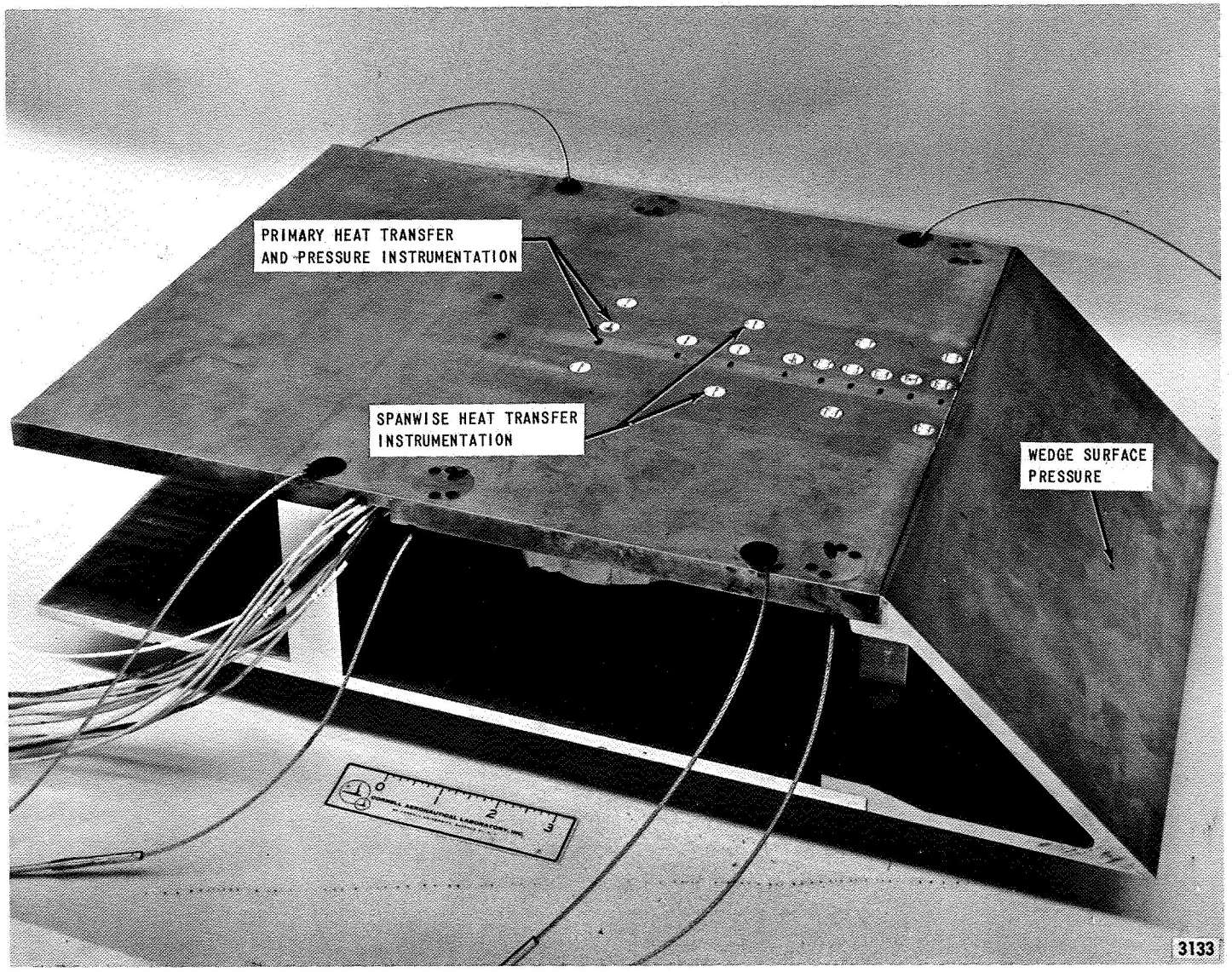

Figure 6 FLAT PLATE MODEL WITH WEDGE LEADING EDGE

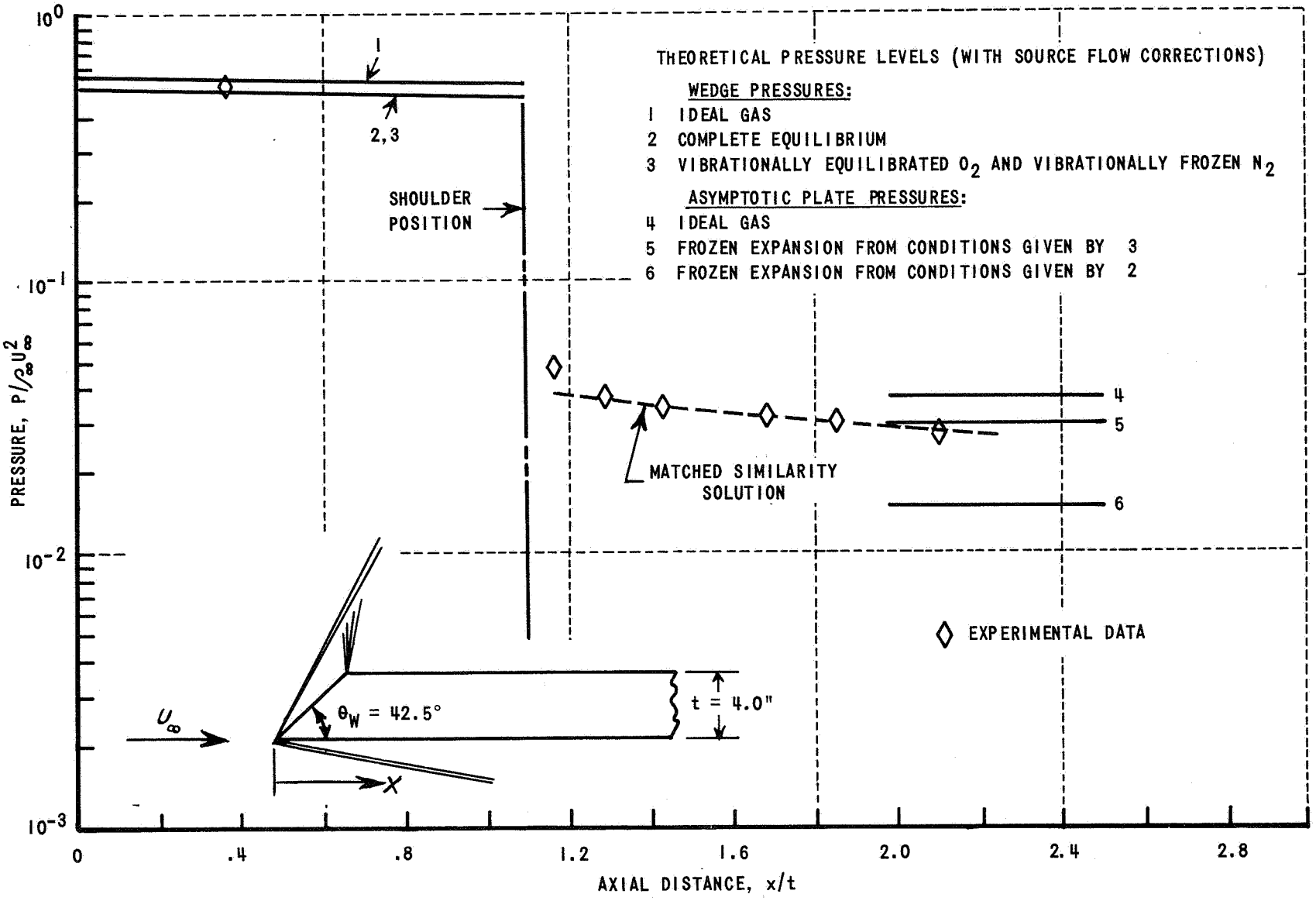

Figure 7 PRESSURE DISTRIBUTION ON A WEDGE-NOSED FLAT PLATE

LOW TEMPERATURE RUN

T_o = 3290°K M_∞ = 15.0 Re_∞/IN = 9210 U_∞ = 9370 FT/SEC

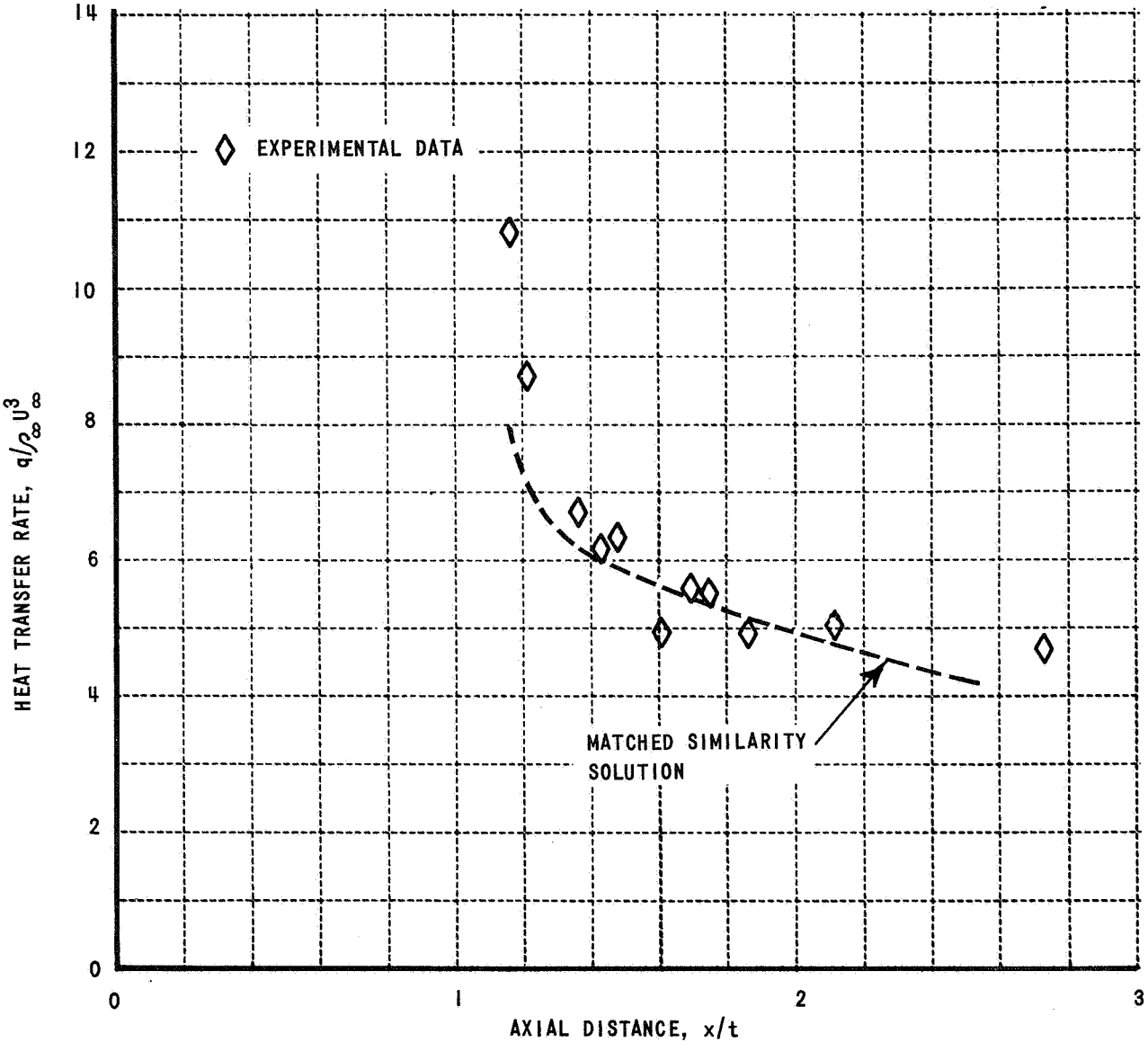

Figure 8 HEAT TRANSFER DISTRIBUTION
LOW TEMPERATURE TEST
T_o = 3290°K M_∞ = 15.0
Re_∞ /IN = 9210 U_∞ = 9370 FT/SEC

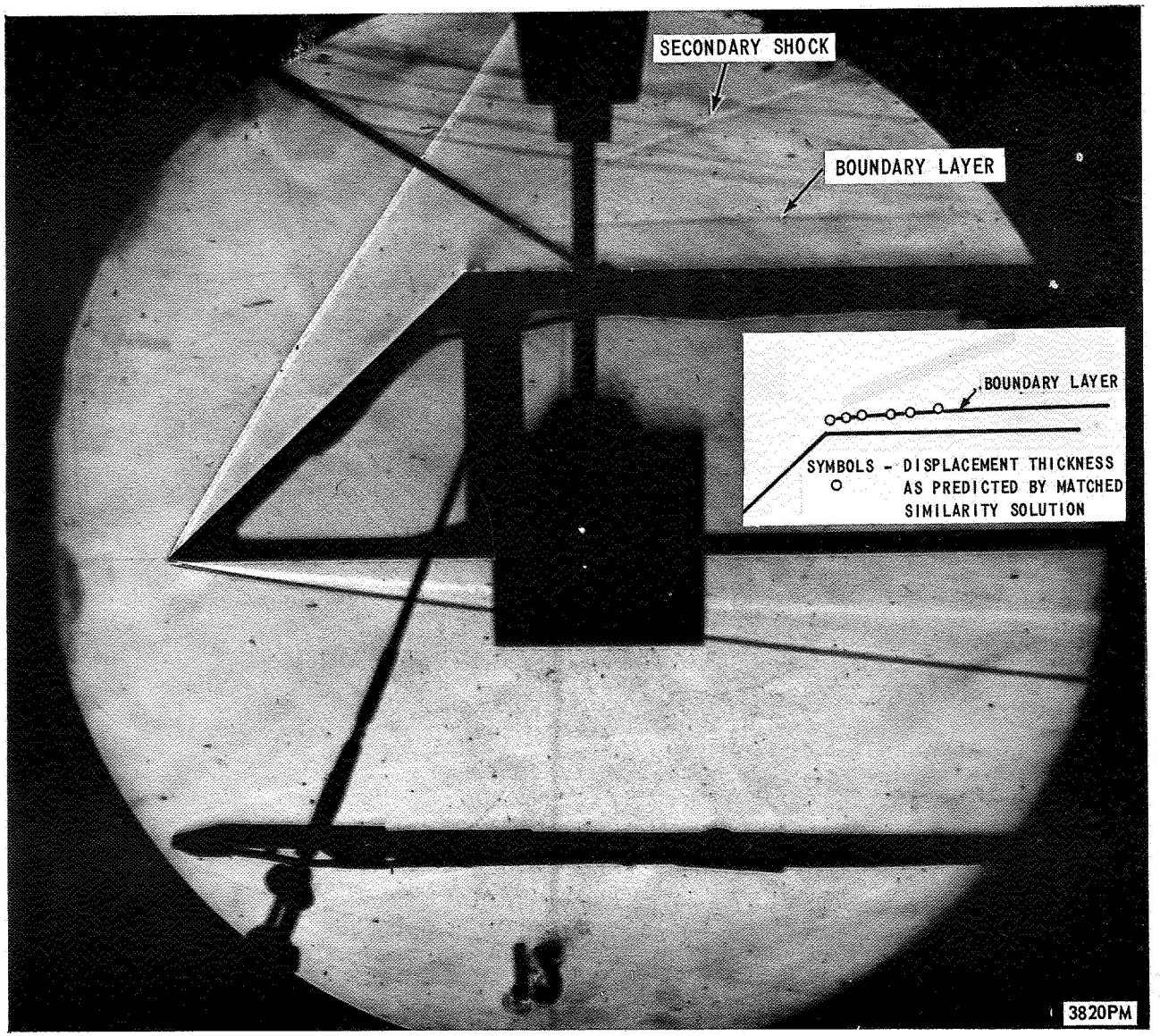

Figure 9 SCHLIEREN PHOTOGRAPH OF WEDGE FLOW FIELD
LOW TEMPERATURE EXPERIMENT
M_∞ = 15.0 Re_∞ = 9210 FT/IN
T_o = 3290 °K U_∞ = 9370 f.p.s.

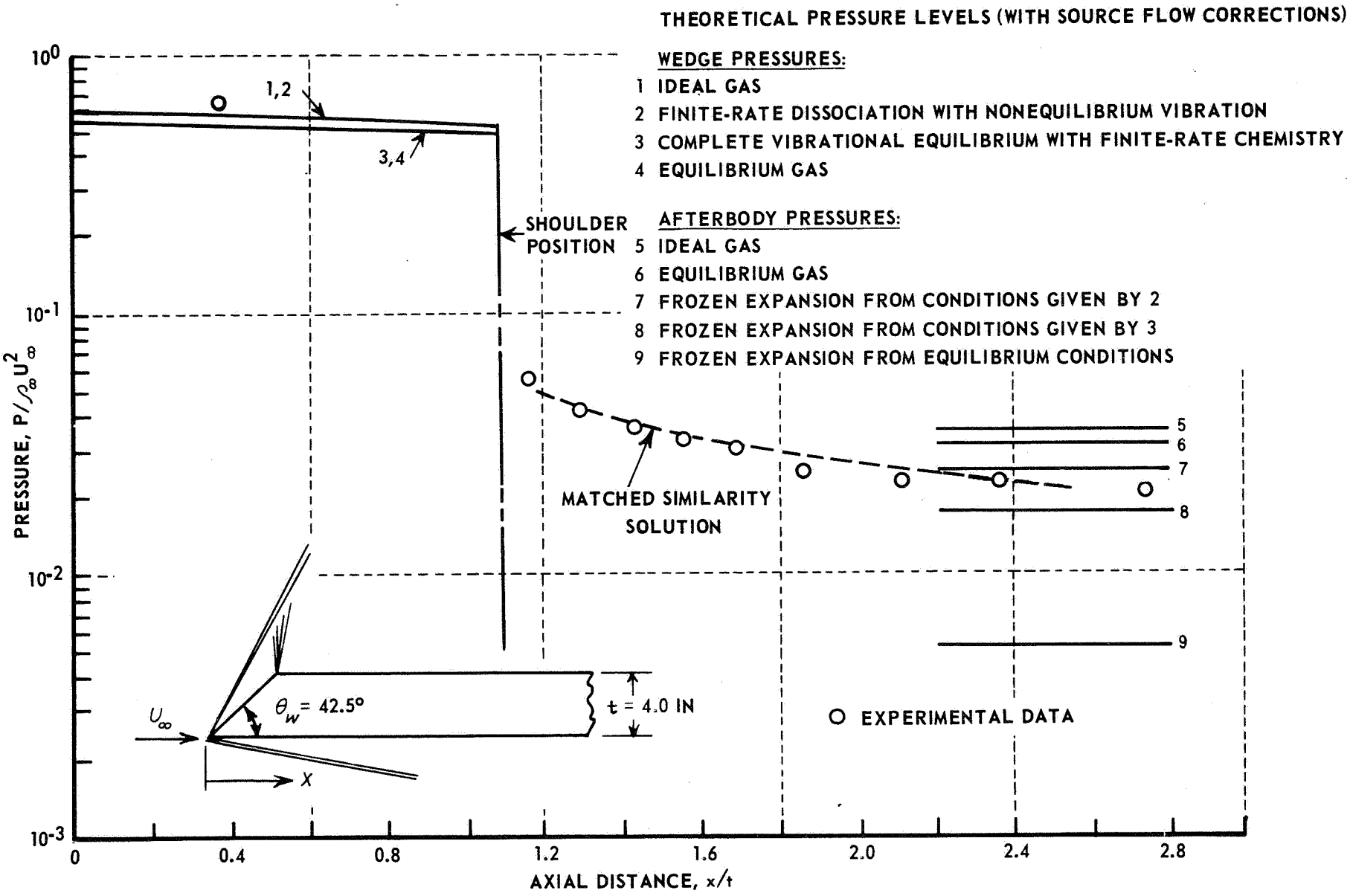

Figure 10 PRESSURE DISTRIBUTION ON A WEDGE-NOSED FLAT PLATE

T_o = 6650°K M_∞ = 16.3 Re_∞/IN = 2680 U_∞ = 14,900 FT/SEC

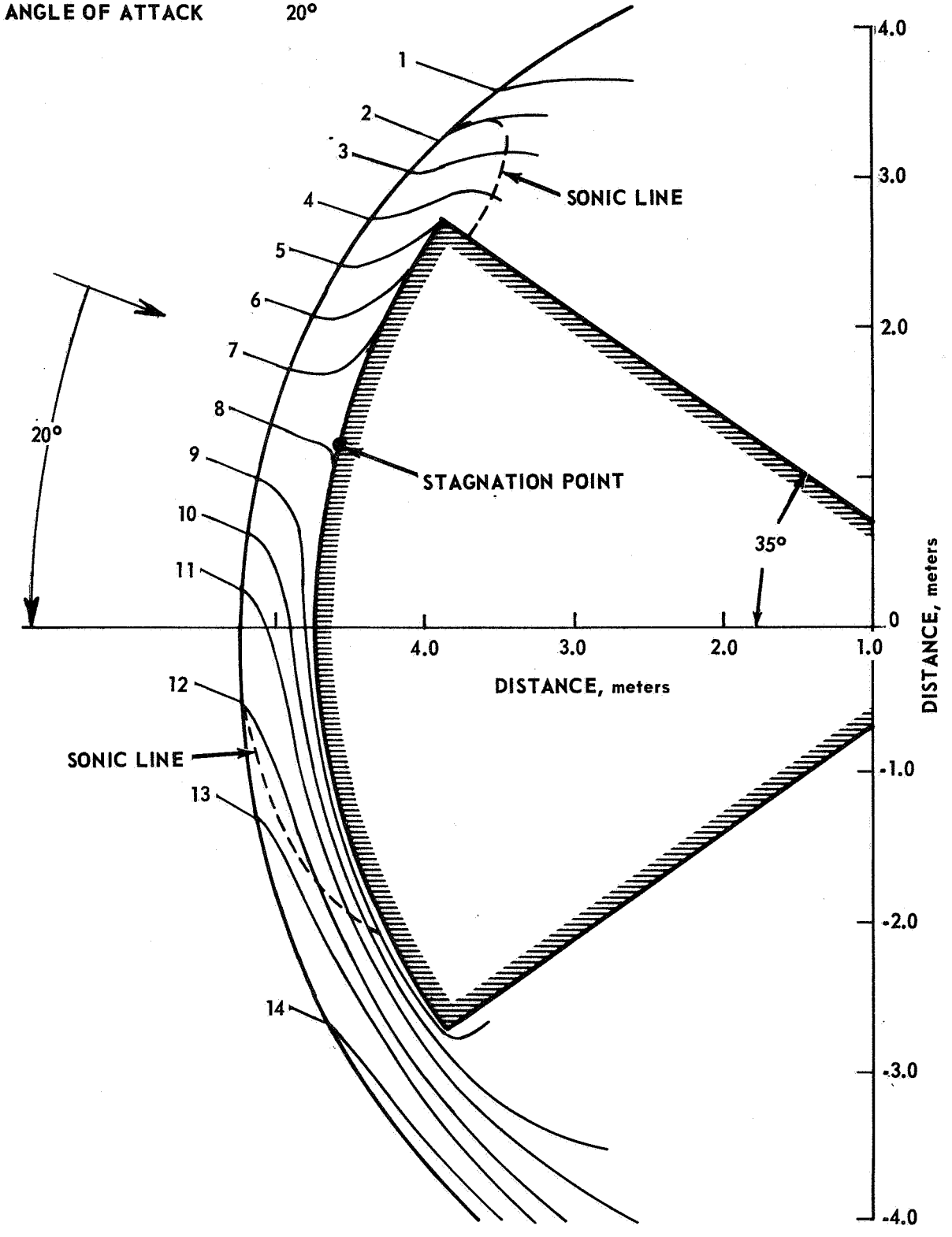

Figure 11 STREAMLINE PATTERN IN THE PLANE OF SYMMETRY

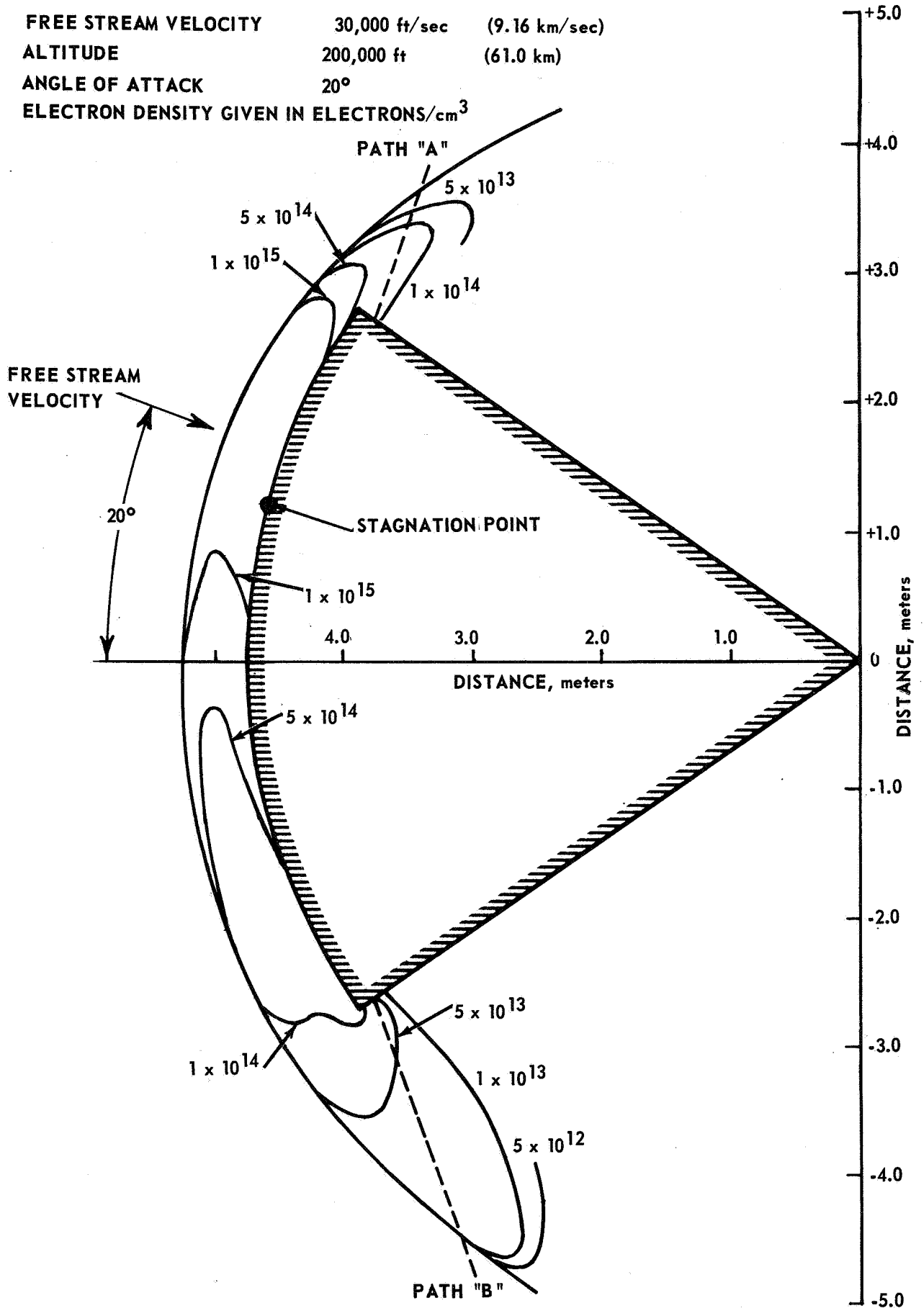

Figure 12 ELECTRON DENSITY DISTRIBUTION IN PLANE OF SYMMETRY

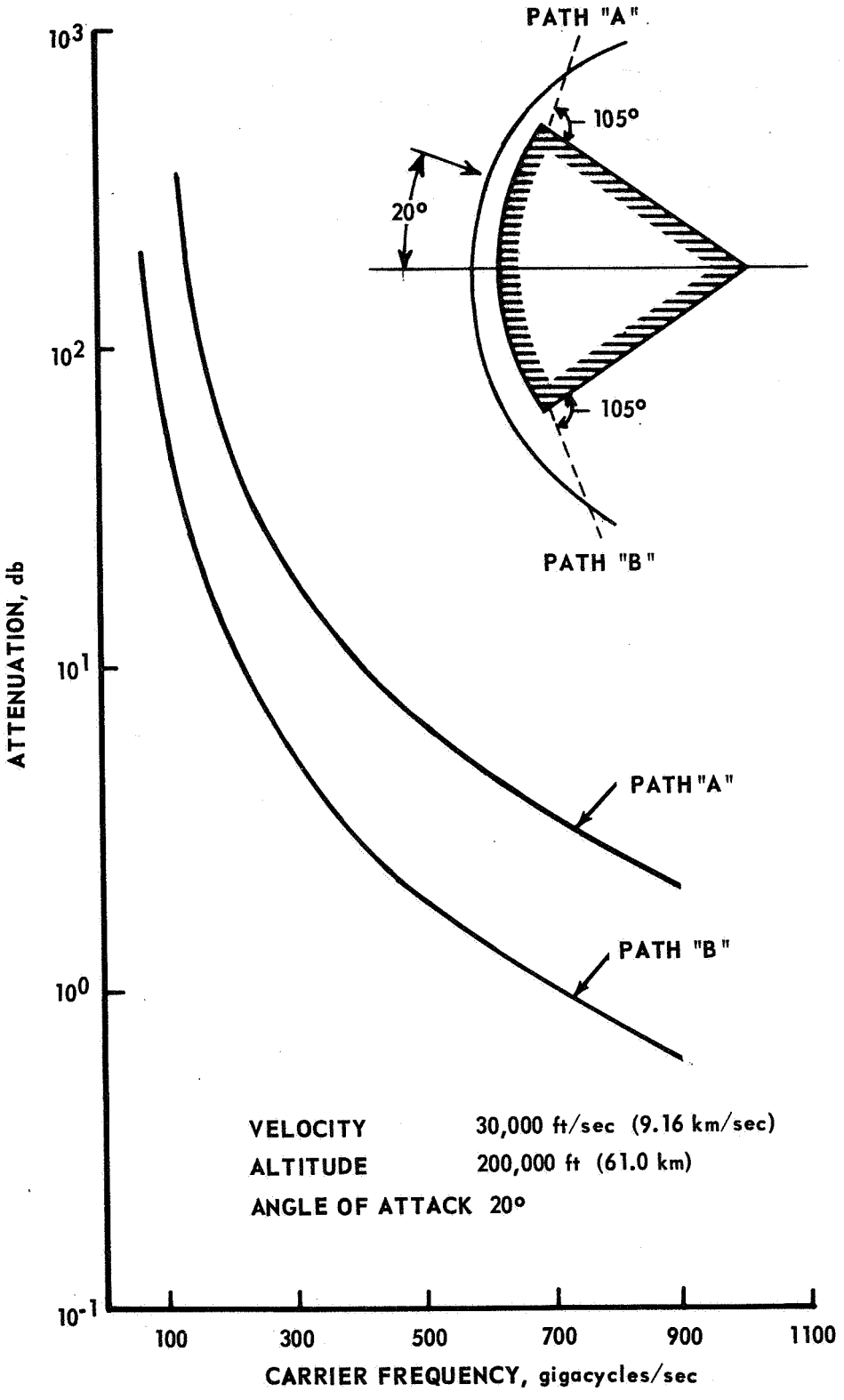

Figure 13 CALCULATED ATTENUATION OF ONE-DIMENSIONAL PLANE WAVES